AIP | APL Materials

Research Update: Molecular electronics: The single-molecule switch and transistor

Kai Sotthewes, Victor Geskin, René Heimbuch, Avijit Kumar, and Harold J. W. Zandvliet

Citation: APL Mater. **2**, 010701 (2014); doi: 10.1063/1.4855775
View online: http://dx.doi.org/10.1063/1.4855775
View Table of Contents: http://scitation.aip.org/content/aip/journal/aplmater/2/1?ver=pdfcov
Published by the AIP Publishing

Research Update: Molecular electronics: The single-molecule switch and transistor

Kai Sotthewes,[1] Victor Geskin,[2] René Heimbuch,[1,a] Avijit Kumar,[1] and Harold J. W. Zandvliet[1]
[1]*Physics of Interfaces and Nanomaterials, MESA+ Institute for Nanotechnology, University of Twente, P.O. Box 217, 7500AE Enschede, The Netherlands*
[2]*Service de Chimie des Materiaux Nouveaux, University of Mons, Mons, Belgium*

(Received 15 October 2013; accepted 11 December 2013; published online 2 January 2014)

In order to design and realize single-molecule devices it is essential to have a good understanding of the properties of an individual molecule. For electronic applications, the most important property of a molecule is its conductance. Here we show how a single octanethiol molecule can be connected to macroscopic leads and how the transport properties of the molecule can be measured. Based on this knowledge we have realized two single-molecule devices: a molecular switch and a molecular transistor. The switch can be opened and closed at will by carefully adjusting the separation between the electrical contacts and the voltage drop across the contacts. This single-molecular switch operates in a broad temperature range from cryogenic temperatures all the way up to room temperature. Via mechanical gating, i.e., compressing or stretching of the octanethiol molecule, by varying the contact's interspace, we are able to systematically adjust the conductance of the electrode-octanethiol-electrode junction. This two-terminal single-molecule transistor is very robust, but the amplification factor is rather limited. [http://dx.doi.org/10.1063/1.4855775]

Molecular electronics is the research field aiming to design and realize elementary electronic devices that rely on single molecules or a small assembly of molecules.[1] In order to realize molecular devices it is of utmost importance to have a firm and detailed knowledge of the properties of a single molecule. This seems trivial, but one has to realize that almost all knowledge we have on molecules is obtained from measurements performed on ensembles of molecules. These measurements provide an averaged result that often includes a term related to the mutual interactions between the molecules.

Since the vast majority of electronic devices rely on transport it is evident that, within the framework of molecular electronics, the most important property of a single molecule is the conductance of a molecule.[2–5] Measuring the conductance of an individual molecule seems at first glance a rather simple task, since one only has to apply a voltage difference across both ends of the molecule and measure the current flowing through it. The problem is that, due to the small size of the molecule, it is very hard to connect it to macroscopic electrical contacts.[6,7] Sophisticated nanoscopic structures and techniques are required to contact a single molecule to the outside world. During the last few decades, several research groups have successfully managed to trap a single molecule between two electrical contacts.[8–22] The most popular technique to contact a single molecule is the quantum mechanical break junction technique, where a nanoscopic junction is realized by controllably opening and closing a narrow metallic constriction.[8,9,21–23] As an alternative, molecules are captured between a substrate and the apex of the tip of a scanning tunneling or atomic force microscope.[5,10–20,24,25]

[a]Author to whom correspondence should be addressed. Electronic mail: r.heimbuch@utwente.nl

Both approaches have their advantages and disadvantages, but scanning probe microscopes have the inherent advantage to image the molecule before it is contacted by the tip.

Once the molecule is properly connected to the outside world, there is yet another problem that hinders a straightforward interpretation of the conductance measurements. This second problem deals with the influence of the electrical contacts on the molecular transport.[6,26] The molecular orbitals of the molecule can hybridize with the electronic states of the contacts leading, in general, to broadening and shifting of the molecular orbitals. The Fermi level of the metal contacts is located between the highest occupied molecular orbital (HOMO) and the lowest unoccupied molecular orbital (LUMO) of the molecule. For small applied voltages and sufficient large HOMO-LUMO gaps the transport mechanism is often coherent non-resonant quantum mechanical tunneling. Charge transport can either occur via the LUMO or HOMO. In the former case we are dealing with electron tunneling, while in the latter case we are dealing with hole tunneling.

In this brief review we will restrict ourselves to the seemingly simple octanethiols. Other than alkanedithiols, which have two identical anchoring groups, monothiols have only one anchoring group, resulting in asymmetric metal-molecule-metal junctions. The latter turns out to be essential in order to achieve true control over the molecular junction, since dithiols are notorious in the sense that (1) once a molecular junction has formed, it is virtually impossible to open the junction again and (2) the affinity of the metallic tip towards dithiols is so large that the tip can easily be decorated with molecules, leading to noisy and low resolution scanning tunneling microscopy images. Despite the simplicity of octanethiols we will show that these molecules can form the basis of elementary molecular devices, such as single molecular switches and transistors.

The experiments were performed in an ultra-high vacuum (UHV) system equipped with an Omicron low-temperature scanning tunneling microscope (LT-STM). The nearly intrinsic Ge(001) samples were thoroughly cleaned with isopropanol alcohol, before inserting them into the UHV system. Subsequently the Ge(001) crystals are first outgassed for at least 15 h at a temperature of about 750–800 K. After cooling down to room temperature the Ge(001) samples are cleaned by cycles of Ar ion bombardment at an energy of 500 eV and annealing at a temperature of 1100 K. After several of these cleaning cycles, the Ge(001) samples were atomically clean and exhibited a well-ordered dimer reconstructed $(2 \times 1)/c(4 \times 2)$ surface.[27]

Next, an equivalent of 0.3–0.5 monolayer of Pt was evaporated on the Ge(001) crystal that was held at room temperature. The Pt was evaporated by resistively heating a high purity Pt (99.995%) wire wrapped around a tungsten (W) wire. After deposition, the sample was annealed at a temperature of 1050 K and then quickly quenched to room temperature before placing it into the STM for imaging. The STM tips we used were either Pt/Ir tips or electrochemically etched W tips. After prolonged scanning of the Pt/Ge(001) surface with a W tip we have the strong impression that the apex of the W tip is decorated with Pt atoms.

Octanethiol molecules (98.5% pure, purchased from Sigma-Aldrich, Germany) are deposited on the Pt modified Ge(001) surfaces by introducing the molecules into a separate UHV chamber for 20–60 s at a pressure of 2.5×10^{-7} Torr via a leak valve. The octanethiols were deposited at room temperature.

Full and constrained geometry optimizations on free alkanethiols were performed at the *B3LYP/6-31g(d,p)* level with *Gaussian 09*.[28] The geometry of alkanethiolate on Pt(111) was optimized by applying periodic boundary conditions on a three-layer-thick platinum system with sufficient distance between the slabs in the normal direction, at the level of density functional theory (DFT) local density approximation (LDA) with a DZP basis set on the molecule and a SZP basis set on the metal (*ATK2008.10* package, quantumwise.org). Even when the relaxation of the upper platinum layer was allowed, its reconstruction was negligible, so for electrostatic potential evaluations all Pt atoms were kept at their crystal positions. The electrostatic potential was calculated classically from the electron density in real space obtained from a periodic calculation, but restricted to one unit cell with the nuclei as point charges. In order to eliminate end effects and to get close to the situation of a single molecule being chemisorbed at a virtually infinite surface, the electron density of a free platinum surface was subtracted from that of the same surface with a molecule. The Pt nuclei were discarded. In this way, the electrostatic potential of the molecule was obtained.

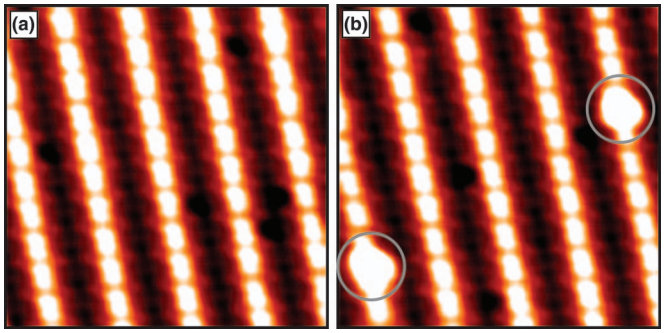

FIG. 1. (a) A STM image of an array of Pt atom chains on a Ge(001) surface recorded at a sample bias of 1.5 V and a tunneling current of 0.5 nA. The image size is 7.5 nm × 7.5 nm. (b) A STM image of an array of Pt atom chains on a Ge(001) surface after the adsorption of a small amount of octanethiol molecules. The adsorbed octanethiolate molecules are almost exclusively found on top of the Pt atom chains. A few octanethiolates are outlined by a circle. The sample bias is 1.5 V and the tunnel current is 0.5 nA. The image sizes are 7.5 nm × 7.5 nm.

In Figure 1(a) a STM image of a Pt-modified Ge(001) surface is shown. In the STM image several Pt atom chains, running from top to bottom, are present. The Pt atom chains are comprised of Pt dimers that have their bond aligned in a direction along the chain. The Pt chains are completely free of kinks and only contain a very low concentration of defects and impurities. Figure 1(b) shows an STM image of a Pt-modified Ge(001) surface on which a small amount of octanethiol molecules are adsorbed. The vast majority of these octanethiol molecules adsorb onto the Pt atom chains. The thiol head of the octanethiol molecule binds to a Pt atom, the hydrogen atom of the SH bond is released and a strong covalent Pt–S bond is formed. At low coverages (octanethiolate molecules are effectively isolated from each other) it is energetically favorable for the carbon tail of the octanethiolate to lie flat down on the substrate. In an attempt to measure the wagging of the carbon tail, we parked the STM tip near the end of the tail of the molecule, disabled the feedback loop of the STM electronics, and recorded the tunnel current as a function of time.[15] A typical current-time trace, recorded at 77 K, is depicted in Figure 2. Initially the tunnel current remained constant around its setpoint value of 1 nA, but after a few seconds the tunnel current jumped to a much higher value of about 11–12 nA (see Figure 2(a)). Several seconds later the current jumped back to its original setpoint value of 1 nA. The large current jump cannot be explained by wagging of the insulating tail of the octanethiolate molecule. The only viable explanation for this dramatic change in the tunnel current is that the tail of the molecule flips up and makes contact with the apex of the STM tip (see Figures 2(b) and 2(c)). The length of the tail is about 1 nm and fits well into the vacuum gap between the substrate and the apex of the STM tip. In the high current state, the current flows through the molecule rather than through the vacuum gap. The measured resistance is about 110–150 MΩ and compares favorably with the resistance of a single octanethiol molecule. A remark is in place here. The conductance, found for a single octanethiol molecule (∼7–8 nS), is about two orders of magnitude larger than the value reported by Haiss *et al.*[29] It is difficult to determine the exact cause of this difference, but we emphasize on the large number of experiments, involving different octanethiol molecules and STM tips, resulting in a remarkable reproducibility of the data.[19] It might be that the contact geometries in both experiments are different, or that the effective tunneling pathway is much shorter in our case. In principle this system behaves as a single molecular switch. However, one should realize that we do not have any control over the switching process in this configuration.

In a second series of experiments we attached the thiol end of the octanethiol molecule to the apex of the STM tip rather than to the substrate.[20] In order to attach the molecule to the tip we preselected an octanethiolate molecule on the substrate, parked the tip on top of the molecule, and picked it up by opening the feedback loop, gradually approaching and once the tip is only a few Ångstroms away from the molecule, we applied a voltage pulse of several volts. After such a picking-up event, we imaged the surface in order to verify whether or not we have really picked up the molecule from the substrate. The success rate for attaching a single octanethiol molecule to the

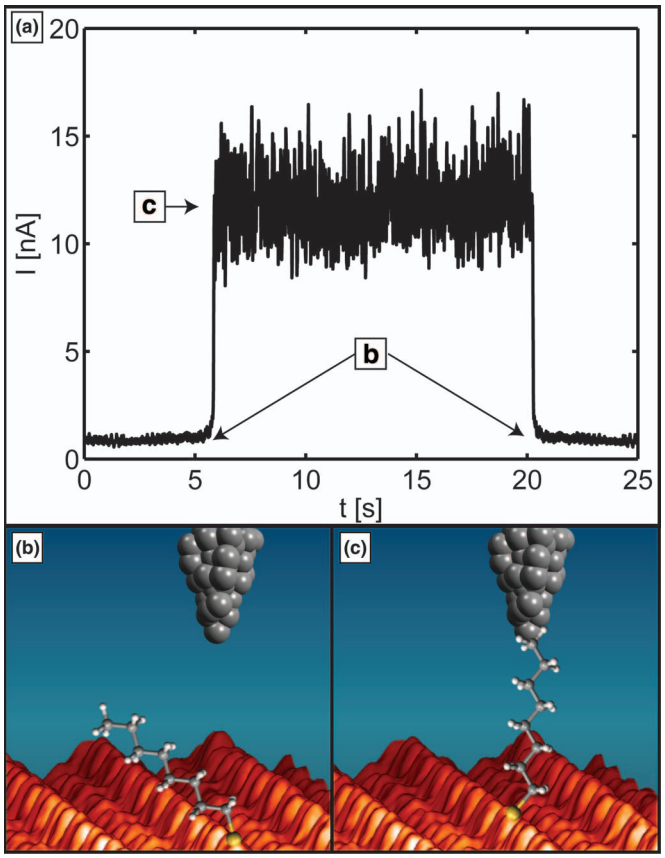

FIG. 2. (a) Current-time trace recorded on top of an octanethiolate molecule at 77 K. The sample bias was 1.5 V and the setpoint current 1 nA. The cartoons in (b) and (c) show the octanethiolate molecule absorbed at a Pt atom chain and an octanethiolate molecule captured between a Pt atom chain and the apex of an STM tip.

apex of the STM is rather low, but once the molecule is picked up by the STM tip it usually remains there for a long time. With the molecule attached to the apex of the tip, we performed a combined current-voltage (I(V)) and current-distance (I(z)) measurements. We recorded I(V) traces from 1.5 V to −1.5 V at different tip-sample separations (see Figure 3). We started with a tip-sample separation slightly larger than the length of the octanethiolate molecule. In steps of 0.05 nm the tip-sample separation was decreased and after a few of these steps the octanethiolate molecule immediately jumped into contact at the initial sample bias of 1.5 V. This opening and closing of the molecular junction is highly reproducible, as indicated by three superimposed series of measurements, shown in Figure 3.

There are few remarks that we need to make here. First, once the molecule jumped into contact the tunnel current was always around 35–40 nA, i.e., about three times larger than when the thiol end of the molecule was attached to the substrate. We interpret this difference using the fact that in the latter case the current flows through one C–C bond less than in the former case. Since the conductance increases by roughly a factor of 3 per C–C bond, it is most probable that the physisorbed contact with the substrate involves two C atoms rather than one. Second, after the molecule has jumped into contact at +1.5 V it always jumped out of contact again once the voltage was lowered to a value near zero bias. It seems counterintuitive that this switching event is triggered by a positive sample bias, i.e., the alkyl end of the chemisorbed octanethiolate is attracted by a positively biased surface. One expects that for a free alkanethiol, the dipole moment vector points from the more negatively charged sulfur atom towards the more positive alkyl group. Prior to the jump into contact with the surface, the octanethiolate is chemisorbed at the Pt decorated W STM tip. Single alkanethiolate molecules on platinum surfaces are more stable in a horizontal geometry,[30] rather than standing upright (as in

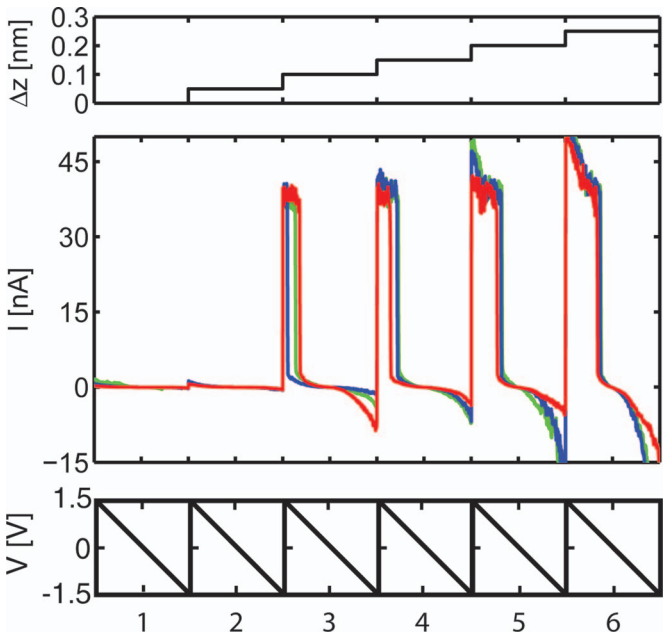

FIG. 3. A set of three I(V) curves (middle graph: red, blue, and green curves) recorded in series, at varying tip-substrate distance with the feedback loop disabled. The top graph shows the relative position of the STM tip with respect to the substrate. The bottom graph shows a series of voltage ramps from +1.5 V to −1.5 V at different substrate-tip separations. Traces in 1 are taken at setpoint values of 0.2 nA and 1.5 V. Traces in 2–6 are recorded at the same setpoint values but, respectively, closer to the substrate.

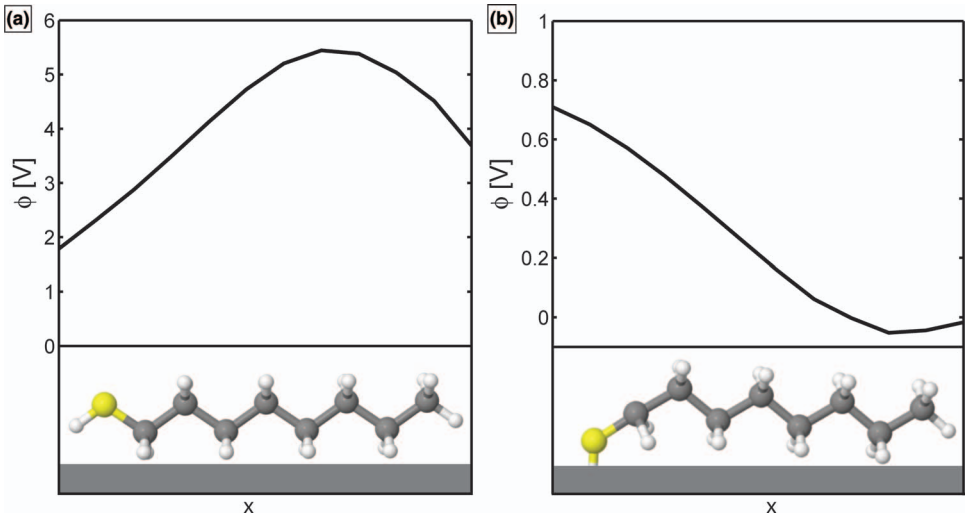

FIG. 4. Free octanethiol molecule (a) and octanethiolate adsorbed on a Pt(111) surface (b). Lower panels: schematic presentation of the position of the molecule with respect to the underlying substrate. Upper panels: electrostatic potentials of molecules at different heights.

a self-assembled monolayer). Jumps into contact can then be due to reorientation of the molecule that stands up from the surface (or tip) into an upright position.

Calculations were done to confirm if there is a charge redistribution within the molecule due to the chemisorbed S-bond. Instead of focusing on dipole moments that can fully characterize neutral electron density distributions as seen from a long distance, we consider here the electrostatic potential created by electrons (whose charge density is taken from a calculation) and nuclei in rather close vicinity to the molecule. Our calculations confirm that for an octanethiol, even at a close

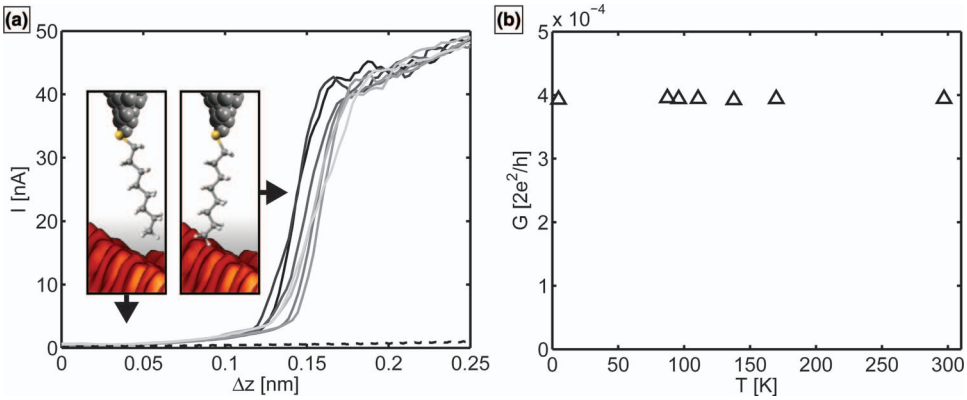

FIG. 5. (a) Current-distance traces recorded without (dotted line) and with (solid lines) an octanethiol molecule attached to the STM tip. T = 77 K, setpoint tunnel current 0.5 nA, and sample bias +1.5 V. (b) Conductance of a single octanethiolate molecule trapped between the apex of a STM tip and a substrate versus temperature.

distance from the surface, but without being chemisorbed, the electrostatic potential, at a distance of a subnanometer distances, is indeed more positive at its methyl end (Figure 4(a)). However, when the molecule jumps into contact, the octanethiolate is chemisorbed at the tip. For an octanethiolate chemisorbed and lying flat on a Pt(111) surface, the electrostatic potential, calculated at planes parallel to the metal surface, shows that it is the thiol end that can be considered as the more positive end of the molecule (Figure 4(b)). Apparently as a consequence of the release of the hydrogen atom and the interaction with the metal, the alkyl end is negatively charged and therefore attracted to a positive electrode.

From the experimental data, supported by calculations, it is immediately clear that this electrode-molecule-electrode configuration behaves as an ideal/deterministic single molecular switch that can be opened and closed at will by carefully adjusting the voltage and the contact's interspace.

In a third series of experiments this molecular switch was used to measure the conductance of a single molecule over a wide temperature range from 4 K all the way up to room temperature.[19] In Figure 5(a) the individual I(z) curves are presented, while in Figure 5(b) the conductance of the single octanethiolate molecule versus temperature is depicted. The conductance was determined shortly after the molecule had jumped into contact with the substrate. All curves are corrected for the temperature-dependent response of the z-piezo. The conductance is temperature independent, indicating that the transport mechanism of the octanethiolate molecule is quantum mechanical tunneling. It should be emphasized that the results presented in Figure 5 are obtained with the same molecule and STM tip.

In order to realize a single-molecule transistor one needs in principle a third electrode which allows to apply a gate voltage that regulates the current flowing from source to drain. As one can imagine, adding a third electrode to a single-molecule junction is far from trivial. Here we propose an alternative scenario, where a separate third electrode is not required. Rather than gating the molecule via a conventional gate electrode, we will vary the conductance of the molecule by mechanical gating, i.e., compressing or stretching the molecule. An electrode-molecule-electrode junction, where one of the electrodes is a STM tip, can easily be mechanically gated by carefully adjusting the tip-sample distance.[31]

In Figures 6(b) and 6(c) current-distance traces are depicted for an octanethiolate molecule, attached to a STM tip (b) and for a normal vacuum gap (c), respectively. In case of the electrode-molecule-electrode system, four curves are presented, where the point of contact is changing from 0.16 nm to 0.19 nm. The current signal is a result of the z-piezo displacement of the tip, presented in Figure 6(a). In case of the vacuum junction (see Figure 6(c)), the tunnel current scales exponentially with tip-sample distance. Initially, a similar distance dependence is also observed for the junction with an octanethiolate attached to the tip (see Figure 6(b)), but once the molecule jumps into contact with the substrate, the tunnel current increases linearly with decreasing tip-sample distance. We will

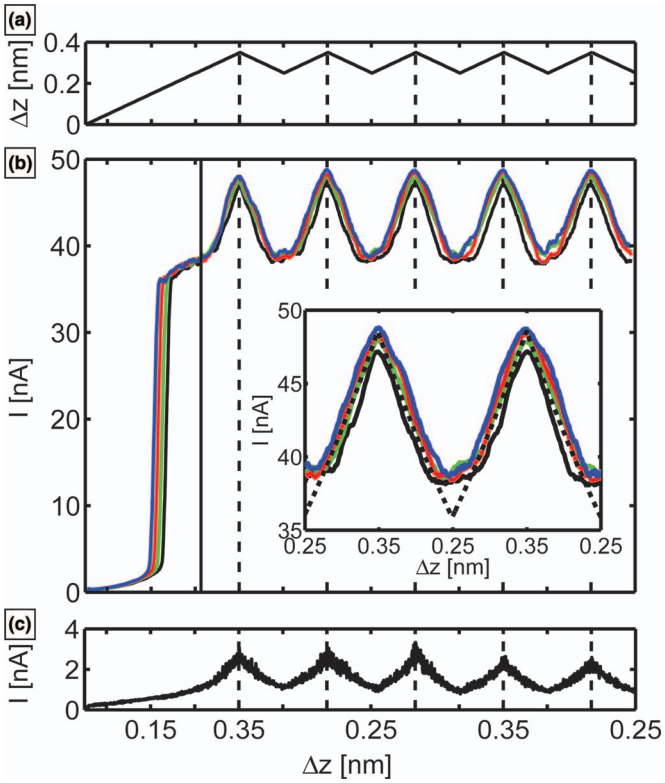

FIG. 6. (a) Relative displacement of the z-piezo (Δz) with respect to a well-defined set point (1.5 V and 0.25 nA); (b) current (I)-distance (z) traces of a single octanethiol molecule junction for different points of contacts; and (c) I(z) trace of a vacuum junction. All I(z) traces are recorded at 77 K. The vacuum junction exhibits an exponential behavior which is a hallmark for tunneling. The molecular junction initially shows the same exponential behavior, until the molecule jumps into contact (here: blue: 0.16 nm, red: 0.17 nm, green: 0.18 nm, and black: 0.19 nm). Upon further reducing the contact's interspace the conductance first marginally increases (left of the black solid line, regime 1) followed by a steeper, but still non-exponential, increase (right of the solid black line, regime 2). The dashed line (inset) refers to a model that involves a tunable image charge effect. We assume that at $\Delta z = 0.25$ nm the electrode-electrode separation is 1.1 nm.

refer to this first linear portion of the current-distance curve as regime 1 (left of the black solid line). After a compression of about 100 pm a pronounced kink in the current vs. distance curve is observed. In this second regime, regime 2, the current still increases linearly with decreasing tip-sample distance, albeit with a substantially larger slope. Since we do not observe an exponential dependence of the current with varying tip-substrate separation, we have to exclude that, in regime 1 as well as regime 2, the molecule is physically compressed or that the molecule slides along one of its contacts.

To elucidate what possibly leads to the existence of two, rather than one linear regime, we consider, with help of quantum-chemical modeling, the conformation of an octanethiolate molecule upon compression. The most stable configuration of alkanes is, of course, all-trans (fully extended) and the first conformational gauche effect defect is about 24 meV higher in energy, according to state-of-the-art calculations.[32] Given that our experiments are performed at 77 K ($kT \approx 6.6$ meV), we can safely assume that the molecule is initially in its all-trans conformation. In our calculations, we start from this fully relaxed conformation and re-optimize the geometry by imposing a shorter molecular length (in practice, the sulfur–last hydrogen distance in the octanethiol). We find that the conformation remains all-trans-like (all the C–C–C–C torsion angles are approximately 180°), the entire backbone is bent, and the molecular energy increases until the contacts interspace is shortened by $\Delta z \approx 65$ pm (red curve in Figure 7). At this point, the somewhat extended conformation, bearing a single gauche-defect (one torsion angle is approximately 60°), becomes more stable than the bent all-trans conformation, i.e., the alkane chain adopts a kink resulting into a shortening of the

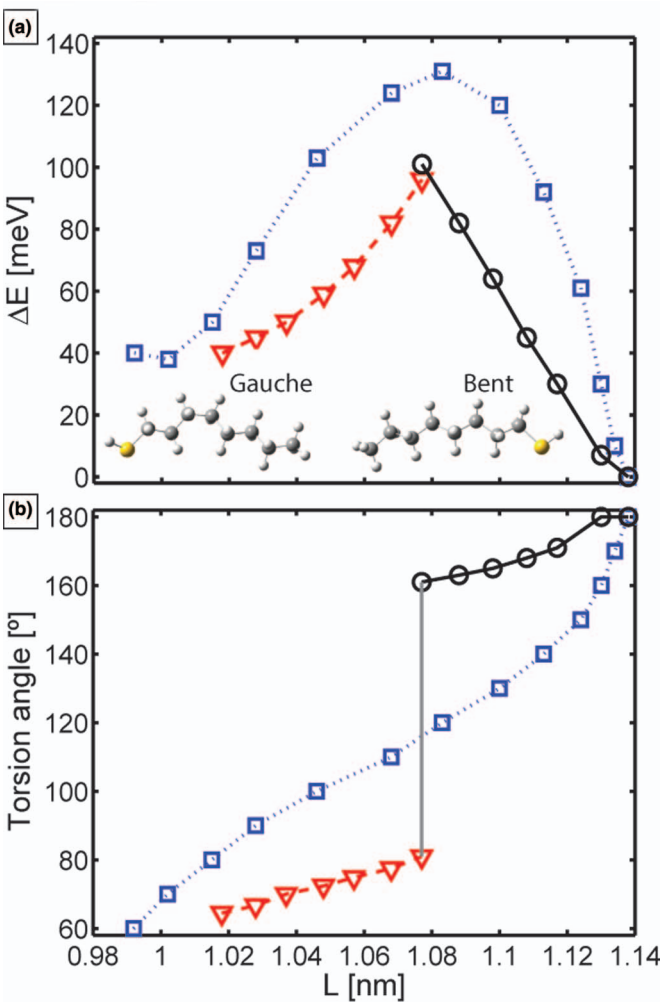

FIG. 7. Calculated conformational changes of an octanethiol molecule upon compression (B3LYP/6-31g(*d*,*p*)). Initially the octanethiol molecule remains in its lowest energy all-trans conformation (black curve), until after a compression of about 0.065 nm the formation of a gauche defect becomes energetically favourable (red curve). The blue curve, for the sake of comparison, shows the torsion angle scan (one torsion angle imposed, all the rest is optimized).

projected length of the molecule along its central axis (the black curve in Figure 7). Note that this qualitative stepwise conformation transition takes place within the same range of compression as in the experiment. Therefore, we suggest, that the linear regimes 1 and 2 refer to different molecular conformations namely, the all-trans conformation at small compressions and the gauche defect conformation at larger compressions, respectively.

In spite of varying the contact's interspace, electron transport occurs predominantly through the bonds of the molecule, and since all the covalent bond lengths remain essentially unaltered as the molecule is bending and twisting, an exponential current-distance dependence is indeed not expected. A remark concerning this scenario would be in order here. While, as already noted, in the bent all-trans conformation compression increases the energy, the formation of a gauche defect would lead to spontaneous shrinking of the molecule, as the energy decreases until the equilibrium for the gauche-defect conformation is attained: the contact could then be lost. As this is not observed in the experiment, we need to postulate that the alkyl end remains attached to the metal, probably due to the applied bias voltage.

The reason for the observed linear dependence in both conductance regimes can be understood by an image charge effect; due to a reduction of the tip-sample separation, the effective barrier height

that the electrons (or holes) encounter is reduced. The effect of mechanical gating is significantly larger in regime 2 than in regime 1, which we ascribe to the reduction of the effective barrier width when the molecule undergoes the bent all-trans to gauche defect transformation. For the remainder of the article we mainly focus on regime 2.

The height of a tunnel barrier is a key parameter determining the decay rate of the wave function of the electrons traversing the barrier. For a small vacuum gap between two metal electrodes, the height of the tunnel barrier is determined by the work functions of both metals. When a potential is applied across the two electrodes, the resulting electric field distorts the potential barrier. For a junction with a width s (in this experiment equal to the length of the molecule L in the gauche configuration (L ≈ 1.1 nm)) and an applied voltage V, the potential barrier at position x is given by

$$\phi_{eff} = \phi_0 - eV\frac{x}{s}. \tag{1}$$

Here the presence of an image force potential has been disregarded. The effect of the image potential is a reduction of the effective trapezoidal barrier height, resulting in an increase of the current flow between the electrodes. The effective barrier, including the image potential is described by[33,34]

$$\phi_{eff} = \phi_0 - eV\frac{x}{s} - 1.15\frac{e^2 \ln 2}{4\pi\varepsilon_0\varepsilon_r s}\frac{s^2}{x(s-x)}, \tag{2}$$

where ε_0 and ε_r are the permittivity of the vacuum and the relative dielectric constant, respectively. If we assume a symmetric junction with its maximum potential barrier height at $x = 1/2\ s$, we find

$$\phi_{eff} = \phi_0 - \frac{eV}{2} - \frac{1.15e^2 \ln 2}{\pi\varepsilon_0\varepsilon_r s}. \tag{3}$$

The dielectric constant of an octanethiol molecule is 2.1.[35] The effective barrier height for an electrode-octanethiolate-electrode junction is given by

$$\phi_{eff} = \phi_0 - \frac{eV}{2} - \frac{eC}{s}, \tag{4}$$

where $C = 2.18 \times 10^{-9}$ V m. It should be pointed out that for an asymmetric junction the prefactors of the second and third terms of Eq. (4) are slightly different, however the s-dependence remains unaltered. The conductance of the single molecule junction can be written as

$$G = Ae^{\frac{-2\sqrt{2m_e}}{\hbar}L\sqrt{\left(\phi_0 - \frac{eV}{2} - \frac{eC}{s}\right)}}, \tag{5}$$

where G is the conductance of the molecule, A is a constant, m_e is the effective electron mass, L is the length of the molecule, and $\hbar$ is the reduced Planck constant. The effective mass of the electron, for tunneling through alkanethiols, is in the range of 0.16–0.42m, where m is the rest mass of the electron. Here we will take an effective mass of 0.28m as reported by Akkerman *et al.*[33]

In the inset of Figure 6(b) the second linear portion of the current-distance curve is shown in more detail. The solid lines are the experimental data and the dashed line is the proposed model, i.e., Eq. (5). We would like to emphasize that the only adjustable parameter is the prefactor A, since the length of the molecule remains unaltered. The best agreement between the experiment and the model is achieved by taking an effective potential barrier height which varies between 1.7 eV and 1.85 eV upon compression. Due to the relatively small range of compression, i.e., 100 pm, the variation of ϕ_{eff} is linear and amounts to 1.5 meV/pm. In principle, mechanical gating provides a way towards the realization of a two terminal single molecule transistor. This approach is very robust and is reproducible, however the amplification factor is limited.

Figure 6(b) shows four different traces where the point of jump into contact slightly varies from 0.16 nm in steps of 0.01 nm to 0.19 nm. We anticipate that the variation in the jump into contact position is intimately related to the exact adsorption geometry of the molecule at the apex of the STM tip. Interestingly, the molecule always has to be compressed by 0.1 nm before the bent all-trans to gauche defect transformation occurs (see Figure 8(a)). In addition, also the actual value of the maximum in conductance, which always occurs at $\Delta z = 0.35$ nm, depends critically on the exact

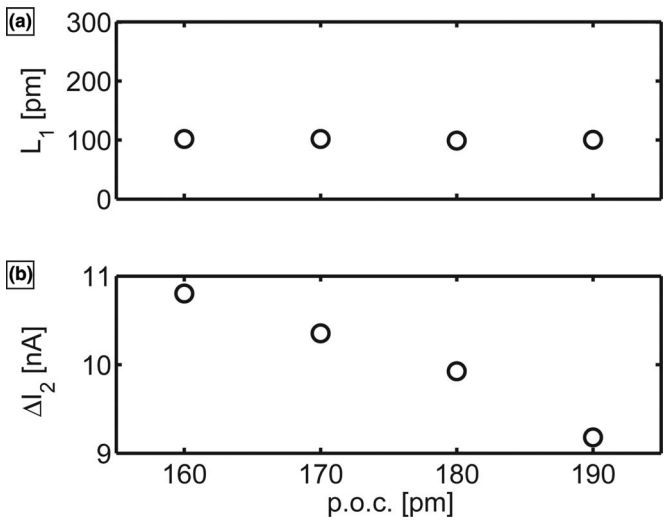

FIG. 8. (a) The length of regime 1 (the linear part in the current versus distance after jump into contact) versus the point of contact and (b) the amplitude of the triangular current modulation as a function of the point of contact (p.o.c).

position at which the molecule jumps into contact. The latter makes sense since a molecule that jumps into contact at 0.16 nm (0.19 nm) transforms from the bent all-trans to the gauche defect conformation at 0.26 nm (0.29 nm) and can thus be compressed by 0.09 nm (0.06 nm). The amplitude of the triangular modulation of the current (ΔI_2) as a function of the point of contact is plotted in Figure 8(b). As expected the amplitude of the triangular modulation of the current decreases when the molecule jumps into contact later. The slope, i.e., $\Delta G/\Delta z$, for regime 2 remains constant and does not depend on the point of contact.

We have systematically studied the transport through a single octanethiolate molecule, trapped between the apex of the tip of a scanning tunneling microscope and a substrate. We have shown that we can controllably attach and detach the molecule to the substrate by adjusting the bias voltage and separation between tip and substrate. This configuration behaves as a perfect single molecular switch, which has an "on" and "off" state. In the "on" state we have measured the conductance of the molecule from 4 K all the way up to room temperature. The conductance of the octanethiol molecule is temperature independent revealing that the transport mechanism is quantum mechanical tunneling. The conductance of the molecule can be controllably adjusted by varying the contact's interspace. The change in conductance of the molecule upon mechanical gating can be explained by a tunable image charge effect. This image charge effect results into a decrease of the tunnel barrier height of 1.5 meV/pm. In principle this single-molecule junction behaves as a two-terminal single-molecule transistor, where the gate electrode is replaced by a mechanical gate.

The amount of control over the molecule junction, we have demonstrated here, will open yet another door into understanding and realization of molecular electronics.

We would like to thank the Dutch Organization for Scientific Research (NWO/CW ECHO.08.F2.008) and the Dutch Organization for Fundamental Research (FOM, 11PR2900 and 10ODE01) and the Interuniversity Attraction Poles Programme (P7/05) initiated by the Belgian Science Policy Office for financial support.

[1] A. Aviram and M. A. Ratner, Chem. Phys. Lett. **29**, 277 (1974).
[2] R. L. McCreery, Chem. Mater. **16**, 4477 (2004).
[3] H. B. Akkerman and B. de Boer, J. Phys. Condens. Matter **20**, 013001 (2008).
[4] S. Karthäuser, J. Phys. Condens. Matter **23**, 013001 (2011).
[5] S. Guo, G. Zhou, and N. J. Tao, Nano Lett. **13**, 4326 (2013).
[6] K. W. Hipps, Science **294**, 536 (2001).
[7] H. J. W. Zandvliet, Chimia **66**(1–2), 52–55 (2012).
[8] R. H. M. Smit, Y. Noat, C. Untiedt, N. D. Lang, M. C. van Hemert, and J. M. van Ruitenbeek, Nature (London) **419**(6910), 906–909 (2002).

[9] L. T. Cai, M. A. Cabassi, H. Yoon, O. M. Cabarcos, C. L. McGuiness, A. K. Flatt, D. L. Allara, J. M. Tour, and T. S. Mayer, Nano Lett. **5**, 2365 (2005).
[10] J. Reichert, R. Ochs, D. Beckmann, H. B. Weber, M. Mayor, and H. von Löhneysen, Phys. Rev. Lett. **88**, 176804 (2002).
[11] W. Haiss, C. S. Wang, I. Grace, A. S. Batsanov, D. J. Schiffrin, S. J. Higgins, M. R. Bryce, C. J. Lambert, and R. J. Nichols, Nat. Mater. **5**, 995 (2006).
[12] L. Venkataraman, J. E. Klare, I. W. Tam, C. Nuckolls, M. S. Hybertsen, and M. L. Steigerwald, Nano Lett. **6** (3), 458 (2006).
[13] G. Meszaros, S. Kronholz, S. Karthäuser, D. Mayer, and T. Wandlowski, Appl. Phys. A **87**, 569 (2007).
[14] R. Temirov, A. Lassise, F. B. Anders, and F. S. Tautz, Nanotechnology **19**, 065401 (2008).
[15] D. Kockmann, B. Poelsema, and H. J. W. Zandvliet, Nano Lett. **9**, 1147 (2009).
[16] L. Lafferentz, F. Ample, H. Yu, S. Hecht, C. Joachim, and L. Grill, Science **323**, 1193 (2009).
[17] E. Leary, M. T. Gonzalez, C. van der Pol, M. R. Bryce, S. Filippone, N. Martin, G. Rubio-Bollinger, and N. Agrait, Nano Lett. **11**, 2236 (2011).
[18] C. Toher, R. Temirov, A. Greuling, F. Pump, M. Kaczmarski, G. Cuniberti, M. Rohlfing, and F. S. Tautz, Phys. Rev. B **83**, 155402 (2011).
[19] R. Heimbuch, H. R. Wu, A. Kumar, B. Poelsema, P. Schon, J. Vancso, and H. J. W. Zandvliet, Phys. Rev. B **86**, 075446 (2012).
[20] A. Kumar, R. Heimbuch, B. Poelsema, and H. J. W. Zandvliet, J. Phys. Condens. Matter **24**, 082201 (2012).
[21] C. Bruot, J. Hihath, and N. J. Tao, Nat. Nanotechnol. **7**, 35 (2012).
[22] M. L. Perrin, C. J. O. Verzijl, C. A. Martin, A. J. Shaikh, R. Eelkema, J. H. van Esch, J. M. van Ruitenbeek, J. M. Thijssen, H. S. J. van der Zant, and D. Dulic, Nat. Nanotechnol. **8**, 282 (2013).
[23] D. Xiang, H. Jeong, D. Kim, T. Lee, Y. J. Cheng, Q. L. Wang, and D. Mayer, Nano Lett. **13**, 2809 (2013).
[24] T. Huang, J. Zhao, M. Peng, A. A. Popov, S. F. Yang, L. Dunsch, and H. Petek, Nano Lett. **11**, 5327 (2011).
[25] C. M. Guedon, H. Valkenier, T. Markussen, K. S. Thygesen, J. C. Hummelen, and S. J. van der Molen, Nat. Nanotechnology **7**, 305 (2012).
[26] G. Wang, T. W. Kim, H. Lee and T. Lee, Phys. Rev. B **76**, 205320 (2007).
[27] H. J. W. Zandvliet, Phys. Rep. **388**, 1 (2003).
[28] M. J. Frisch, G. W. Trucks, H. B. Schlegel *et al.*, Gaussian 09, Revision A.02, Gaussian Inc., Wallingford, CT, 2009.
[29] W. Haiss, S. Martin, E. Leary, H. van Zalinge, S. J. Higgins, L. Bouffier, and R. J. Nichols, J. Phys. Chem. C **113**, 5823 (2009).
[30] M. A. F. Addato, A. A. Rubert, G. A. Benitez, M. H. Fonticelli, J. Carrasco, P. Carro, and R. C. Salvarezza, J. Phys. Chem. C **115**, 17788 (2011).
[31] K. Sotthewes, R. Heimbuch, and H. J. W. Zandvliet, J. Chem. Phys. **139**, 214709 (2013).
[32] D. Gruzman, A. Karton and J. M. L. Martin, J. Phys. Chem. A **113**, 11974 (2009).
[33] J. G. Simmons, J. Appl. Phys. **34**, 2581 (1963).
[34] J. G. Simmons, J. Appl. Phys. **34**, 1793 (1963).
[35] H. B. Akkerman, R. C. G. Naber, B. Jongbloed, P. A. van Hal, P. W. M. Blom, D. M. de Leeuw, and B. de Boer, Proc. Natl. Acad. Sci. U.S.A. **104**, 11161 (2007).